J Mater Sci: Mater Electron (2011) 22:838–842
DOI 10.1007/s10854-010-0222-8

The effect of CuO doping on the microstructures and dielectric properties of $BaTiO_3$ ceramics

**Tao Li · Kun Yang · Renzhong Xue ·
Yuncai Xue · Zhenping Chen**

Received: 31 July 2010 / Accepted: 25 September 2010 / Published online: 8 October 2010

Abstract $(1-x)$ $BaTiO_3/x$CuO ceramic pellets with $x = 0$, 0.2, 0.4, 0.6, and 0.8% respectively were prepared by the traditional solid-state reaction method. The effect of CuO doping on the microstructure and dielectric properties of $BaTiO_3$ ceramics has been investigated. SEM and XRD results at room temperature show that the grain size grows with the increase of CuO content under the same sintering conditions and the crystal structure undergoes the mixed phases (pseudocubic/tetragonal) to tetragonal phase transition with the growth of grain size. Regular shape grains with average grain size ~ 2 μm are detectable in the specimens as CuO dopant content adds up to 0.8% and the crystal structure has completely changed into tetragonal phase. The permittivity increases markedly for CuO dopant content $x = 0.2 \sim 0.4\%$ and the dielectric loss decreases significantly after being doped by CuO and down to a minimum value for $x = 0.8\%$. In addition, the permittivity and dielectric loss display a good stability in a broad frequency range comparing that of pure $BaTiO_3$ ceramics.

1 Introduction

$BaTiO_3$ is a ubiquitous electronic ceramic and $BaTiO_3$-based ceramics have been widely used in electronic industrial products, such as ceramic capacitors, sensors and thermal components, as well as micro-electronic systems and so on. Many theoretical and experimental studies aimed at preparing techniques, modeling and characterizing have been carried out [1–4]. However, some of the properties of pure $BaTiO_3$, such as narrow working temperature-stable range, large dissipation factor et al., limit its usefulness in certain areas. To improve the dielectric behavior of $BaTiO_3$, many metal-oxides have been used to be additives. Metal-oxides-doped $BaTiO_3$ ceramics have been found to possess a significant improvement in dielectric properties, as well as an interesting dielectric relaxation behavior [5–7]. In addition, the normal sintering temperature of $BaTiO_3$ based ceramics is about 1,300 °C. To lower the sintering temperature of modified $BaTiO_3$ ceramics has been strongly desired in the industrial fields. Some metal oxides can not only be used as a sintering agent to reduce the sintering temperature of $BaTiO_3$ ceramics, but also can be used as an additive to improve the properties of $BaTiO_3$ ceramics [8, 9]. Yang [10] has investigated the relation between the ratio of CuO/BaO additive and the grain growth of $BaTiO_3$ ceramics. The effect of the sintering aid SiO_2 on the dielectric properties of $BaTiO_3$- or $BaTiO_3$-based ceramics has been examined by Lee et al. [11]. CuO as a sintering agent for $BaTiO_3$-based ceramics has been studied by Derling et al. [12]. The findings have shown that CuO can act as an effective sintering agent for $BaTiO_3$-based ceramics, functioning both as low melting flux former and as internal subsector for microwave sintering. But its effect on the dielectric properties has not been studied specifically. In this paper, a small amount of CuO has been used as a sintering agent for $BaTiO_3$ ceramics and its effect on the microstructures and dielectric properties of $BaTiO_3$ ceramics will be analyzed and discussed.

2 Experimental procedure

The pure $BaTiO_3$ powder was prepared using the traditional solid-state reaction method. All the raw materials

---

T. Li · K. Yang · R. Xue · Y. Xue · Z. Chen (✉)
Department of Technology and Physics, Zhengzhou University
of Light Industry, Zhengzhou 450002,
People's Republic of China
e-mail: hnlt529@126.com

used were analytical grade: $BaCO_3$ (>99.5%), TiO_2 (>99.8%). Reagent-grade $BaCO_3$, TiO_2 were weighed by the stoichiometric ratios. Mixed powders were ball- milled in alcohol using zirconia balls in sealed agate vessel for 8 h. The slurry was dried and then calcined at 1,150 °C in air for 3 h. XRD patterns show that the calcined powder was basically formed into a single $BaTiO_3$ phase. The calcined $BaTiO_3$ powder was then mixed in terms of the formula $(1 - x)$ BaTiO3/xCuO, with $x = 0$, 0.2, 0.4, 0.6, and 0.8% respectively. The obtained mixed powder was remilled for 4 h and granulated by adding PVA, then pressed into pellets (150 MPa) with a diameter of 12.0 mm and thickness of 2.0 mm. Finally the pellets were sintered in air at 1,100 °C for 3 h. In order to measure the electric properties, silver paste was painted on the polished samples as the electrodes and fired at 600 °C for 15 min.

X-ray diffraction (XRD) with Cu K- radiation ($\lambda = 0.1541$ nm) was performed to examine the phase constitution of specimens at room temperature. Microstructural characterization of the ceramics was carried out in a scanning electron microscope (SEM) at 15 kV, with the samples coated by a Pd–Au film. The dielectric properties of the pellets were determined using an Agilent 4294A Precision Impedance Analyzer from 40 Hz to 110 MHz. The ferroelectric properties were measured using the Radiant Precision Workstation Materials Analyzer (RADIANT) while the pellets were put into silicon oil. Densities of the sintered pellets were measured using the Archimedes method.

3 Results and discussions

The relative densities of the sintered specimens are 90.13, 94.15, 94.22, 95.84 and 96.63%, corresponding to CuO dopant content $x = 0$, 0.2, 0.4, 0.6 and 0.8% (the theoretical density of pure $BaTiO_3$ is 6.02 g/cm^3 [13]). It is obvious that the density increases observably with the increase of CuO dopant content. This suggests that CuO functioning as low melting flux former can be used as an effective sintering agent for $BaTiO_3$ ceramics contributing to the growth of grains at lower sintering temperature and improving the densification of $BaTiO_3$ ceramics.

Figure 1 shows SEM photos of the morphologies and grains of $(1 - x)$ $BaTiO_3/x$CuO ceramics. It can be found that the grain growth is not obvious; the average grain size of the specimen with $x = 0$ is $\sim$ 0.45 μm and it has not changed significantly for $x = 0.2$ and 0.4%. However, the grains begin to present the trend of continuous growth for $x = 0.4\%$ as shown in the white circle in Fig. 1. For $x = 0.6\%$, the grain size increase sharply and many shapeless grains have appeared. It is interesting that a large number of regular shape grains are presented and the average grain size is $\sim$2 μm as CuO dopant content adds up to 0.8%, which indicates that a small amount of CuO dopant can effectively reduce the sintering temperature contrasting $\sim$1,300 °C, the sintering temperature of BaTiO3 ceramics by the traditional solid-state reaction method.

Figure 2 shows X-ray diffraction patterns of the pellets doped with different contents of CuO dopant. It can be found that the positions and the intensities of the diffraction peaks are similar and no second phases can be observed. The XRD patterns also demonstrate the single $BaTiO_3$ phase compared with the standard PDF database [JCPDF File No. 520626]. However, the gradually splitting of the (0 0 2)/(2 0 0) peaks around 45° of 2θ in Fig. 2b with the increase of CuO dopant content manifests that the crystal structure undergoes the mixed phases (pseudocubic/tetragonal) to tetragonal phase transition with the growth of grain size and it has completely changed into tetragonal phase for $x = 0.8\%$. This can be deduced by the results of SEM, because when the grain size is lower than 700 nm, the lattice of $BaTiO_3$ ceramic changes from tetragonal to pseudocubic [14].

The variations of permittivity and dielectric loss of $(1 - x)$ $BaTiO_3/x$CuO ceramics at room temperature measured at selected frequencies versus CuO content x have been given in Fig. 3. It can be found that the permittivity ε_r increases markedly for $x = 0.2 \sim 0.4\%$ and the highest value can be obtained for $x = 0.4\%$, then decreases as x amounts to $0.6 \sim 0.8\%$. Nevertheless, it is higher than that of the specimen with $x = 0$. The dielectric loss tan δ decreases significantly after being doped by CuO and down to a minimum value for $x = 0.8\%$. For the samples with $x = 0.2$, 0.4, 0.6 and 0.8%, the dielectric loss tan δ is about 0.0125, 0.0136, 0.0067 and 0.0065 respectively at 1 kHz. Compared with that of the $BaTiO_3$ specimen, 0.0373, it is reduced by 66.5, 63.5, 82.0 and 82.6%.

The frequency dependence of permittivity ε_r and dielectric loss tan δ of $(1 - x)$ $BaTiO_3/x$CuO ceramics at room temperature measured has been given in Fig. 4. Obviously, after being doped by CuO, the dielectric properties of the specimens have been improved greatly. It can be found that all the specimens doped by CuO show a permittivity of $\varepsilon_r > 2200$, the maximum of the specimen with $x = 0$ below 10^6 Hz and the curves display more stable plateaus with the increase of CuO additive content in a broad frequency range, then followed by a strong drop for about 10^7 Hz. The dielectric loss tan δ of the specimen with $x = 0$ at low frequencies (below $\sim$10 kHz) is larger and has much stronger frequency dependence than that of CuO-doped specimens. It increases gradually after 10^5 Hz and rises suddenly at about 10^7 Hz for all the samples, corresponding to the strong drop of the permittivity ε_r at about 10^7 Hz.

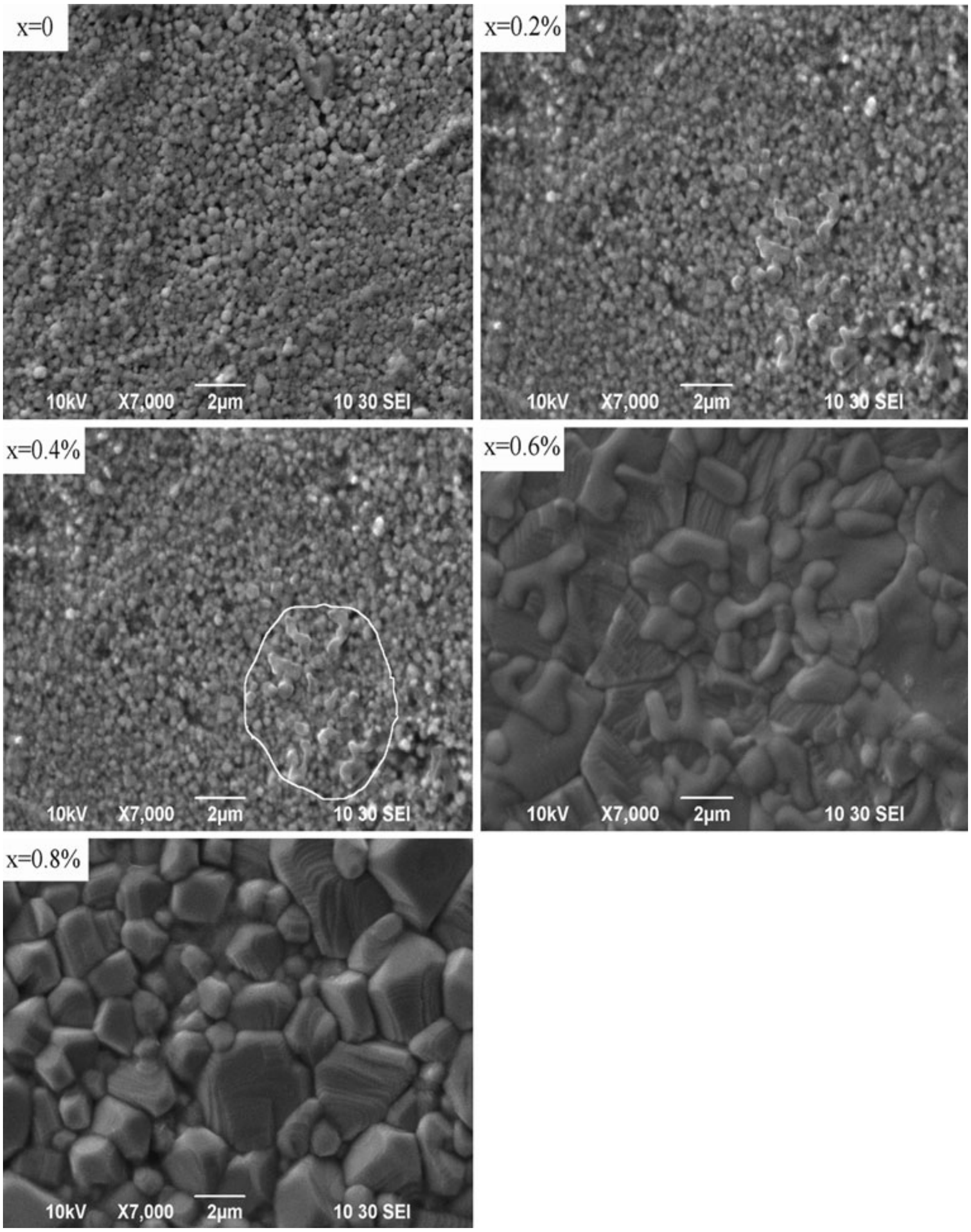

Fig. 1 SEM photos of (1 − x) $BaTiO_3/xCuO$ ceramics

Because the porosity is not an important parameter that affects the ε_r when the relative density is above 90% ρ_t and there is not much relation between the variety of dielectric properties of ceramics and the relative density of $BaTiO_3$/xCuO according to the report [15]. So the variety of dielectric properties of $BaTiO_3$/xCuO ceramics can be ascribed to other factors.

When CuO dopant content is lower, for $x = 0.2$ and 0.4%, during the sintering process most of the copper as acceptor cation Cu^{2+} is distributed at grain boundaries and triple points, which not only improves the concentration of the polarization charge, but also increases the resistivity of grain boundary. This leads to the increase of permittivity ε_r and the decrease of dielectric loss tan δ. However, when CuO dopant content increases to $x = 0.6$ and 0.8%, due to lower melting point, it can promote the growth of grains as an effective sintering aid at lower sintering temperature, which can be seen in the photos of SEM. The grain size development can result in the decrease of permittivity ε_r for $BaTiO_3$ ceramics [16]. In addition, a partly incorporation of Cu^{2+} into the $BaTiO_3$ lattice near the grain boundaries cannot be excluded, which can affect the polarization of electric domains near the grain boundaries and raise the reversal energy of dipoles. Both the above factors acting together lead to a slight decrease of the permittivity ε_r.

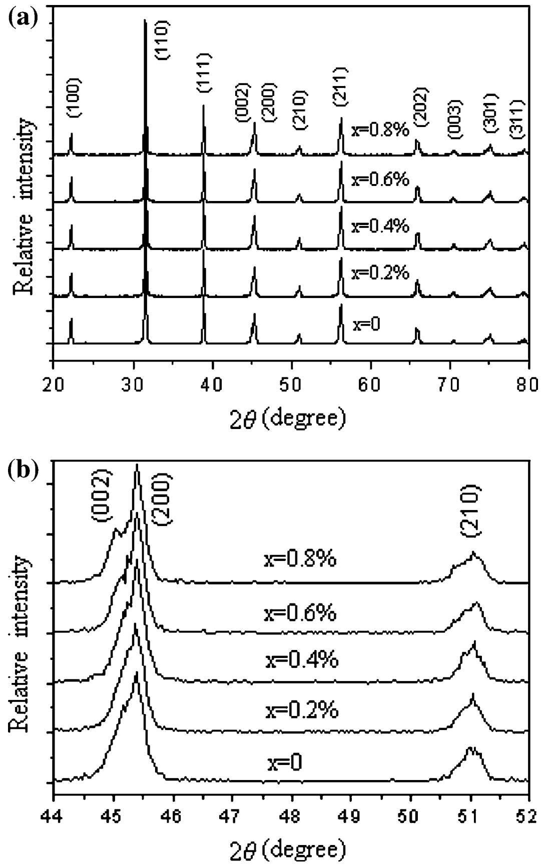

Fig. 2 The X-ray diffraction patterns of (1 − *x*) $BaTiO_3$/*x*CuO ceramics

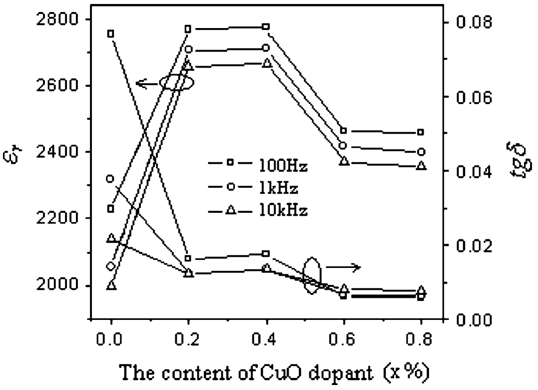

Fig. 3 The permittivity and dielectric loss of (1 − *x*) $BaTiO_3$/*x*CuO ceramics versus CuO content *x* measured at 1 kHz, 10 kHz and 1 MHz

Figure 5 shows the temperature dependence of the dielectric properties measured at 1 kHz for (1 − *x*) $BaTiO_3$/*x*CuO ceramics. The Curie temperature of the specimens is ~109 °C for CuO dopant content $x \leq 0.4\%$, and reaches 114 and 119 °C for $x = 0.6$ and 0.8% respectively due to the growth of grain size. According to the above discussion, the growth of grain size corresponds to the phase transition of the crystal structure from the mixed phases (pseudocubic/tetragonal) to tetragonal with the increase of CuO dopant content, which leads to the rise in the Curie temperature (the temperature for the crystal structure from tetragonal to cubic). In addition, it can also be found that the temperature dependence of permittivity (ε_r) of the specimens decreases gradually with the increase of CuO dopant content below 80 °C. It can be ascribed to a partly incorporation of Cu^{2+} into the $BaTiO_3$ lattice near the grain boundaries, which affects the polarization of electric domains near the grain boundaries and raises the reversal energy of dipoles, and so the lower energy of thermal vibration is not enough for the dipoles to reverse.

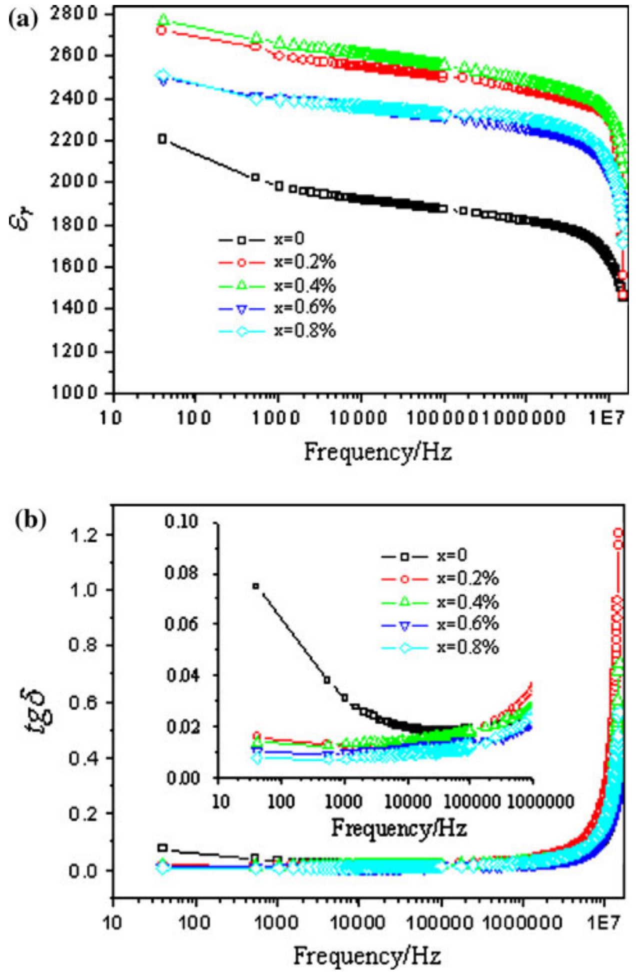

Fig. 4 Frequency dependence of the permittivity (**a**) and dielectric loss (**b**) of (1 − *x*) $BaTiO_3$/xCuO ceramics at room temperature

4 Conclusions

The microstructures of the specimens reveal that the sintering temperature of $BaTiO_3$ ceramic can be reduced

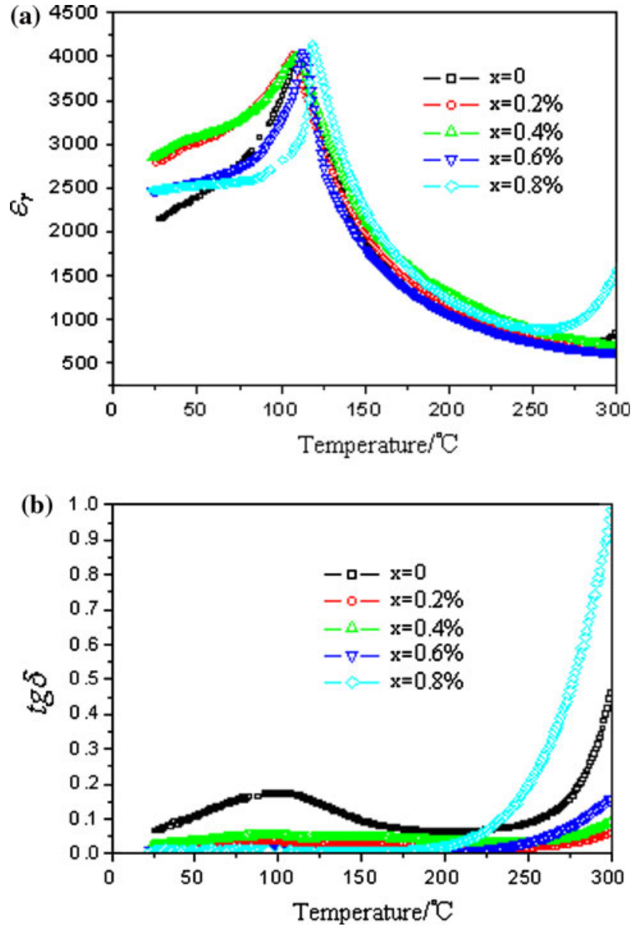

Fig. 5 Temperature dependence of the permittivity (**a**) and dielectric loss (**b**) measured at 1 kHz for (1 − x) $BaTiO_3/xCuO$ ceramics

effectively by a small amount of CuO doping, illustrated by the specimen with CuO dopant $x = 0.8\%$ which has perfect crystal morphology and whose sintering temperature can be reduced by ~200 °C compared with that of pure $BaTiO_3$ ceramics. The grain size of the specimens increases obviously for CuO dopant content $x \geq 0.6\%$; the crystal structure undergoes the mixed phases (pseudocubic/tetragonal) to tetragonal phase transition with the increase of grain size and it has completely changed into tetragonal phase for $x = 0.8\%$. The permittivity increases markedly and the dielectric loss decreases significantly after being doped by CuO. Both the permittivity and dielectric loss present a good stability in a broad frequency range comparing that of pure $BaTiO_3$ ceramics. This is very interesting to improve the dielectric properties of $BaTiO_3$ or $BaTiO_3$-based ceramics.

Acknowledgments This work was supported by National Natural Science Foundation of China (Project No. 10875107), The Natural Science Foundation of Henan (Project No. 82300440080), The Basic Research Plan on Natural Science of the Education Department of Henan Province (Grant No. 2008A140014) and (Grant No. 2010 B140016).

References

1. G.V. Lewis, C.R.A. Catlow, J. Casselton, J. Am. Ceram. Soc. **68**, 555–561 (1985)
2. J.H. Han, D.Y. Kim, Acta Mater. **46**, 2021–2028 (1998)
3. W.S. Cho, J. Phys. Chem. Solids **59**, 659–666 (1998)
4. F.J. Gotor, L.A. Perez-Maqueda, J.M. Criado, J. Eur. Ceram. Soc. **23**, 505–512 (2003)
5. Y. Liu, A.R. West, J. Eur. Ceram. Soc. **29**, 3249–3257 (2009)
6. A. Shukla, R.N.P. Choudhary, A.K. Thakur, D.K. Pradhan, Physica B **405**, 99–106 (2010)
7. R. Köerstein, L. Jäer, M. Zenkner, S.G. Ebbinghaus, Mater. Chem. Phys. **119**, 118–122 (2010)
8. H.-P. Jeon, S.-K. Lee, S.-W. Kim, D.-K. Choi, Mater. Chem. Phys **94**, 185–189 (2005)
9. G. Liu, R.D. Roseman, J. Mater. Sci. **34**, 4439–4445 (1999)
10. F.-C. Yang, Ceram. Int **24**, 341–346 (1998)
11. Y.C. Lee, W. Lu, S.H. Wang, C.H.W. Lin, Int. J. Miner. Metall. Mater. **16**, 124–127 (2009)
12. S. Derling, Th. Müller, H.-P. Abicht, K.-H. Felgner, H.T. Langhammer, J. Mater. Sci. **36**, 1425–1431 (2001)
13. C.-Y. Chen, W.-H. Tuan, J. Am. Ceram. Soc. **83**, 2988–2992 (2000)
14. W. Luan, L. Gao, J. Guo, Ceram. Int **25**, 727–729 (1999)
15. T.T. Fang, H.L. Hsieh, F.S. Shiau, J. Am. Ceram. Soc. **76**, 1205–1211 (1993)
16. M.H. Frey, D.A. Payne, Phys. Rev. B **54**, 3158–3168 (1996)